

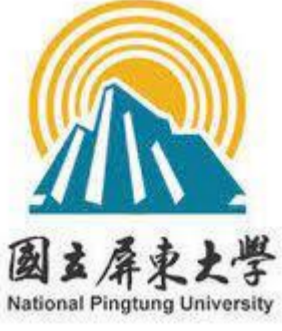
Selective adsorption capacity of $\text{Fe}_3\text{O}_4@\text{C}$ nanoparticles with respect to organic cationic dyes

O.S. Ivanova^{*,1}, I.S. Edelman¹, A.E. Sokolov¹, E.S. Svetlitsky¹, Chun-Rong Lin², Ying-Zhen Chen², Yaw-Teng Tseng²

*e-mail: osi@iph.krasn.ru



¹ Kirensky Institute of Physics, 50/38 Akademgorodok St., Krasnoyarsk 660036, Russia



² Department of Applied Physics, National Pingtung University, Pingtung City 90003, Taiwan

Introduction

In recent years, there has been an avalanche-like increase in the number of publications on the use of the adsorption properties of magnetic nanoparticles (NPs), in particular, magnetite. At the same time, the variety of fields of application is striking in its breadth - chemical, pharmaceutical, food, agricultural, and many others [1]. The variety of uses of magnetite NPs is due to the ability to reliably attach various substances to their surface. Magnetite NPs are attractive objects for creating core-shell structures and modifying their surface in order to create functional properties. The creation of selective adsorption by NPs is invaluable, in some cases to remove certain substances from solutions, and in other cases, for example, medicine, in order to deliver the necessary substances to certain places. Possession a large magnetic moment allows you to control the movement of magnetic particles.

The carbon shell is one of the universal coatings for NPs. It provides exceptional chemical stability and protects the magnetic core from oxidation, prevents agglomeration and allows additional functionalization. High adsorption capacity $\text{Fe}_3\text{O}_4@\text{C}$ NPs along with easy magnetic separation and the possibility the multiple use noted in these works stimulates the search for new technological solutions for further improving the characteristics of adsorbents based on these NPs [2].

This work is devoted to a comparative study of the adsorption capacity of **cationic** (Methylene blue (MB), rhodamine C (Rh C)) and **anionic** (Congo red (CR), methyl orange (MO) and eosin y (EoY)) dyes by Fe_3O_4 and $\text{Fe}_3\text{O}_4@\text{C}$ NPs.

- [1] J.S. Beveridge, J.R. Stephens, M.E. Williams. Annu. Rev. Anal. Chem. 4 (2011) 251.
 [2] M.M. Lima, D.L.P. Macuvelo, et al. J. Adv. Chem. Eng. 7 (2017) 1000172.

Samples characterization

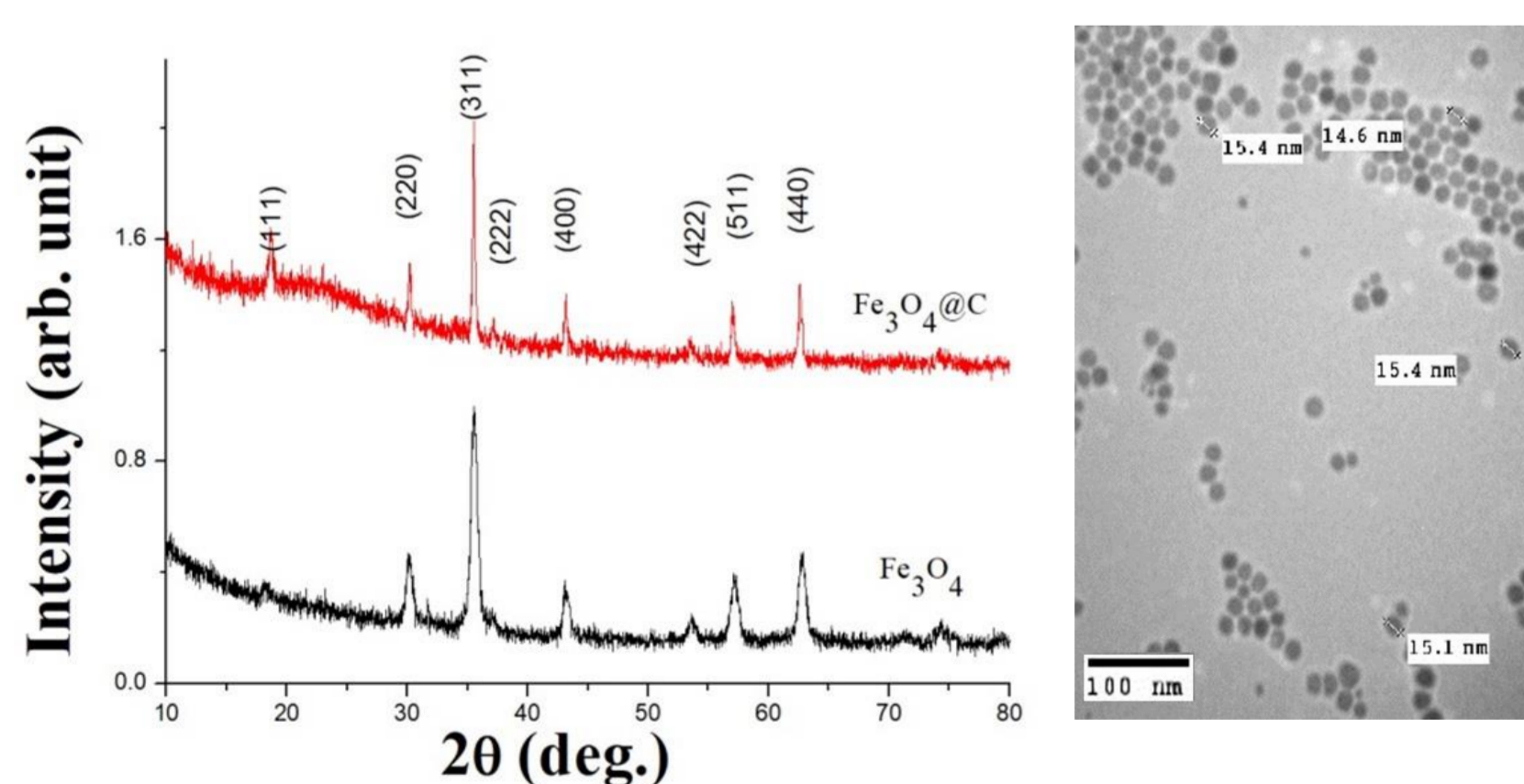


Fig. 1. X-ray diffraction patterns of both samples and TEM image of Fe_3O_4 NPs.

The Fe_3O_4 NPs were nearly spherical crystals with an average diameter of about 15 nm. The most intense X-ray peaks corresponded to the Fe_3O_4 phase (PDF Card # 04-005-4319) in both case.

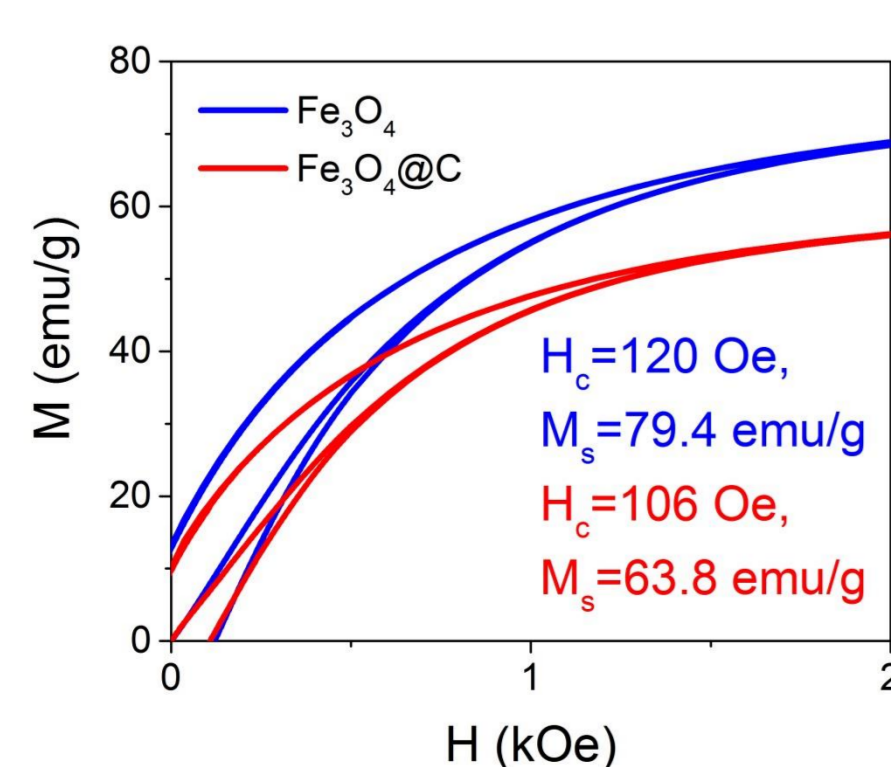


Fig. 2. VSM magnetization curves for Fe_3O_4 and $\text{Fe}_3\text{O}_4@\text{C}$ NPs. The value of saturation magnetization (Ms) is given in the field 15 kOe. The saturation magnetization of bulk magnetite (84 emu/g).

Experiment

Magnetite Fe_3O_4 NPs were obtained from the thermal decomposition reaction of iron-oleate complex. After that, the Fe_3O_4 NPs were mixed with glucose in distilled water by sonication for 15 min was placed in an autoclave for 12 h at 200°C. After cooling to room temperature, the black products were then separated by an external magnetic field and washed several times with water and ethanol (Fig.2). Next, the NPs $\text{Fe}_3\text{O}_4@\text{C}$ were dried at 60°C for 6 hours.

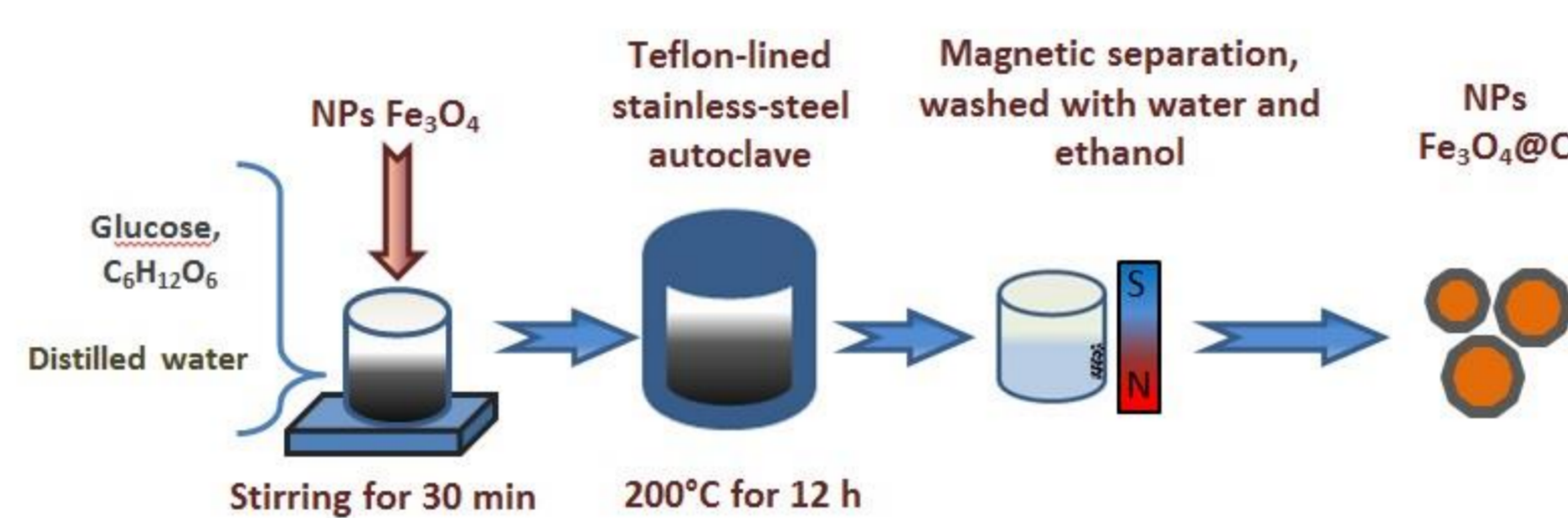


Fig. 2. Schematic illustration of the carbon shell formation on Fe_3O_4 NPs. The equipment used is shown in a simplified manner.

The synthesized NPs were examined with X-ray diffraction, transmission electron microscope (TEM), vibrating sample magnetometer (VSM). Changes in the absorption spectra of the dye solutions were recorded with the UV/VIS circular dichroism spectrometer SKD-2MUF at the wavelength corresponding to the maxima in the spectra of 490 nm for eosin Y, 505 nm for CR, 500 nm for MO and 664 nm for MB.

For the experiment, 3 mg of NPs were dispersed in 1.5 ml aqueous dye solution in an ultrasonic bath for 10 minutes. Then magnetic NPs were separated using magnetic field and measured the optical absorption of the remaining solution. Then the solution was again mixed with NPs, and the described procedure repeated several times (Fig.3).

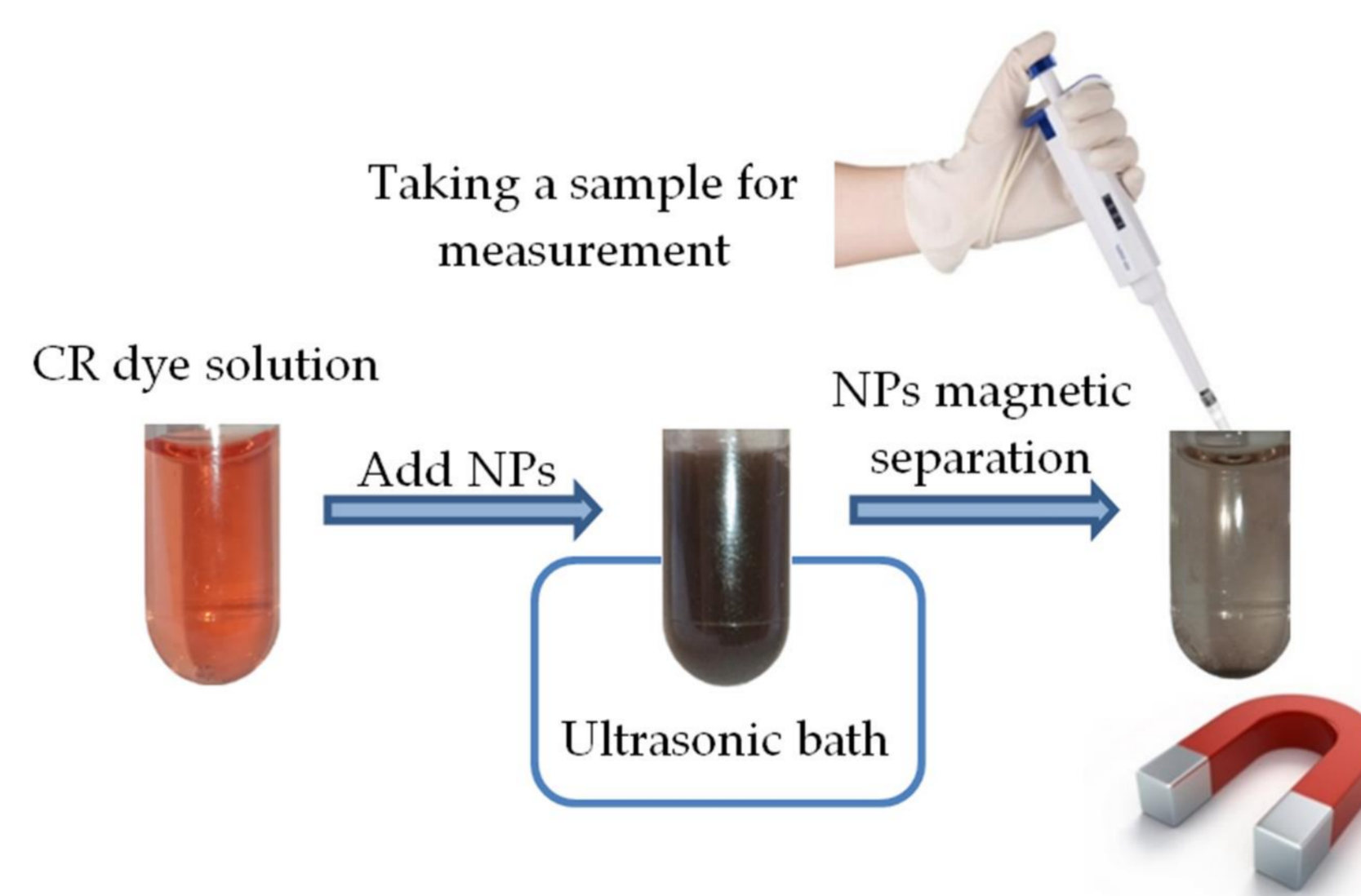


Fig. 3. Schematic picture showing the preparation of a sample to measure the adsorption capacity, using the CR ($C_0 = 30$ mg/L) water solution as an example.

The value of the adsorption capacity of NPs at any point in time, q_t (mg/g) was calculated as follows:

$$q_t = \frac{(C_0 - C_t)V}{m} \quad (1)$$

where C_0 and C_t is the initial and concentration of the dye at any time, V is the volume of the solution; and m represents the weight of the adsorbing NPs introduced into solution.

Acknowledgements: The work was supported financially by Ministry of Science and Technology of Taiwan, Grants MOST № 108-2923-M-153-001-MY3 and № 109-2112-M-153-003-

Adsorption

The $q_t(t)$ dependencies for different dyes are shown in Fig. 1 for the Fe_3O_4 NPs.

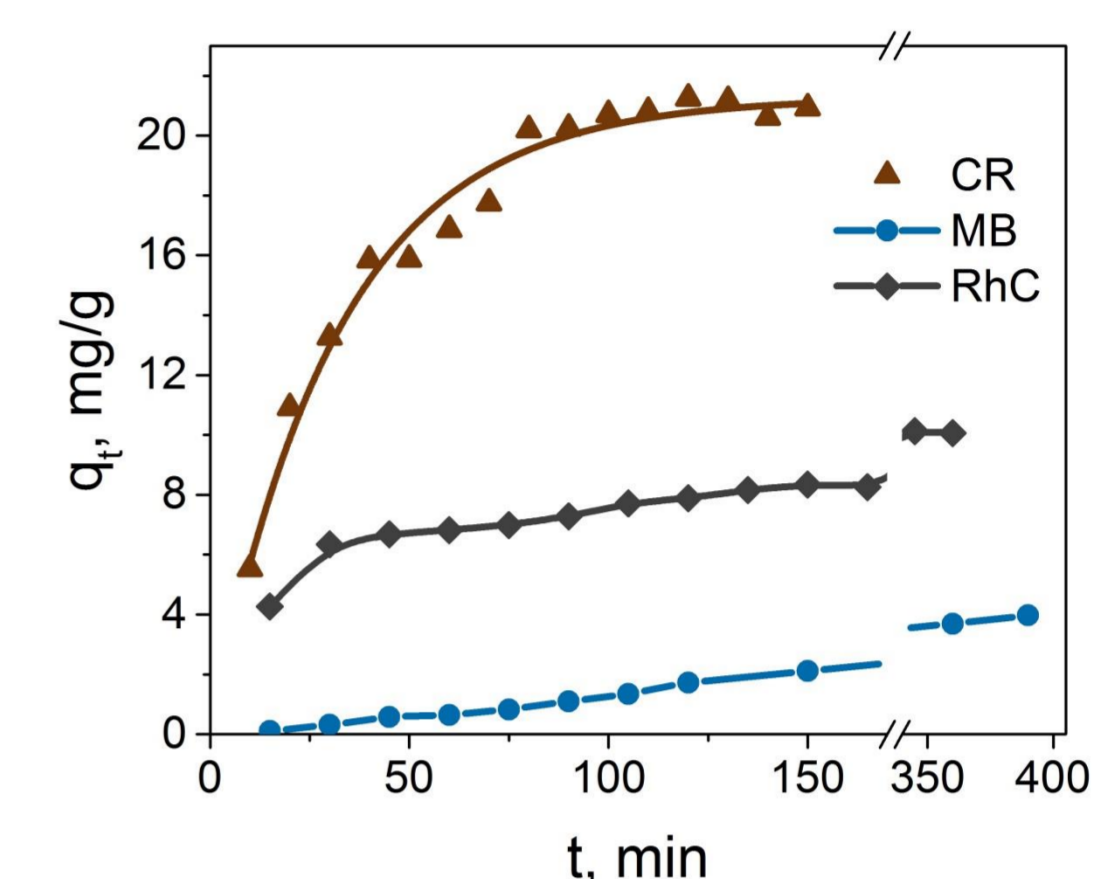


Fig. 4. The effect of contact time on the dye adsorption for Fe_3O_4 NPs. Experimental conditions: $C_0 = 60$ mg/L.

The higher values of the adsorption capacity and the short time to reach the equilibrium value for the CR indicate the preferred absorption of anionic dyes by Fe_3O_4 NPs. The kinetic curve for CP is well described by the pseudo-first order kinetic model, and the isotherm shape is well described by Brunauer-Emmett-Teller (BET) theory isotherm equation for liquid phase adsorption for Case-3 - polymolecular adsorption model. At the same time, up to a dye concentration of 50 mg/L, nanoparticles adsorbed 90 % of the dye, with an increase in the dye concentration up to 200 mg/L, particles adsorbed up to 60 % of the dye.

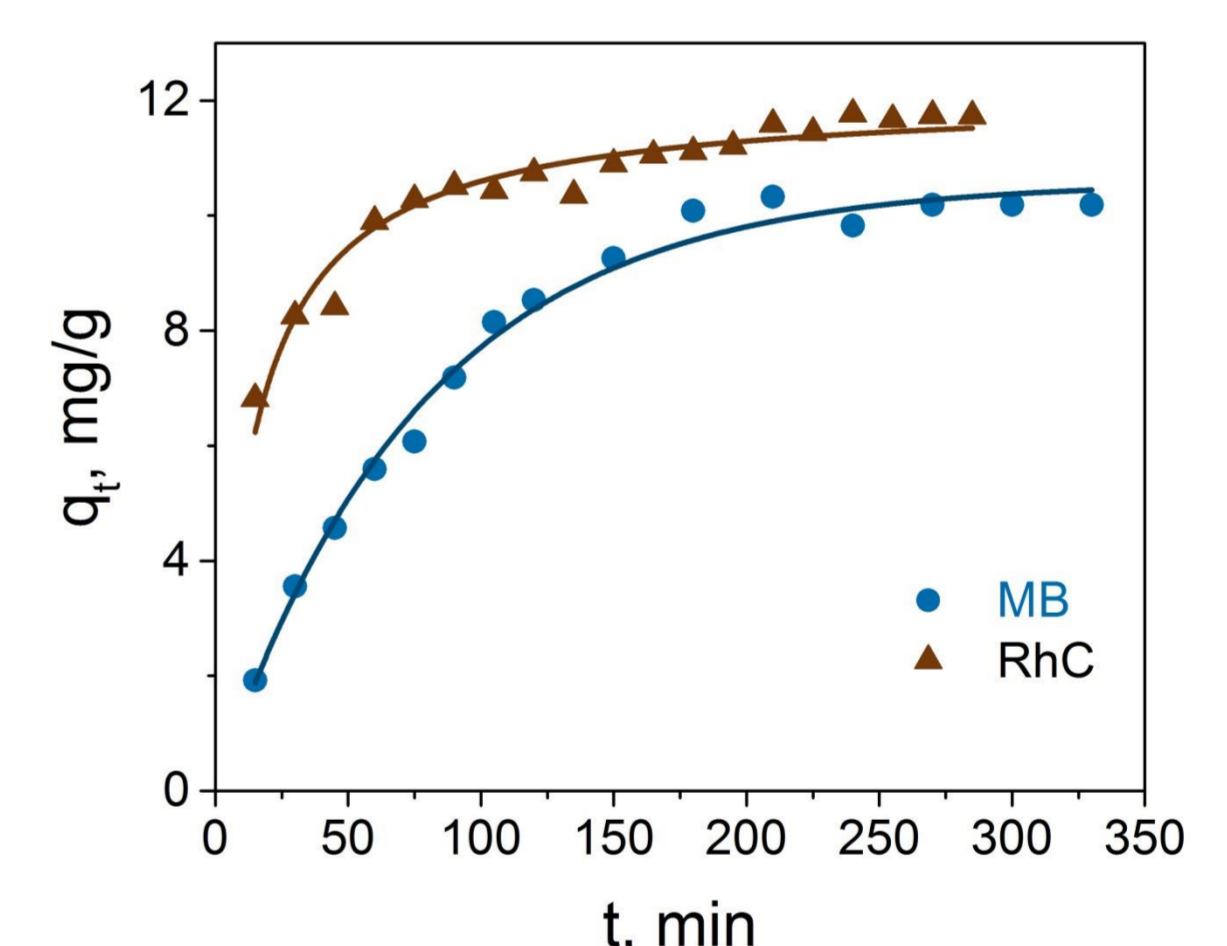


Fig. 5. The effect of contact time on the dye adsorption for $\text{Fe}_3\text{O}_4@\text{C}$ NPs. Experimental conditions: $C_0 = 30$ mg/L.

The adsorption capacity of the core shell $\text{Fe}_3\text{O}_4@\text{C}$ NPs has changed dramatically, NPs have expressed complete indifference to anionic dyes: CR, MO and EoY. The ability to adsorb cationic dyes while improving (Fig. 5). The concentration dependences of the equilibrium value of the adsorption capacity are described by the Langmuir equation, showing the formation of a homogeneous adsorbed monolayer, while the adsorbed molecules do not interact with each other.

Conclusions

The Fe_3O_4 and core-shell $\text{Fe}_3\text{O}_4@\text{C}$ magnetic NPs with an average size of 15 ± 2 nm were synthesized and characterized.

The Fe_3O_4 NPs showed predominant adsorption of anionic dyes. The kinetic data are well described by the pseudo first order kinetic model, and the shape of the isotherm by the BET equation for liquid phase polymolecular adsorption.

The $\text{Fe}_3\text{O}_4@\text{C}$ NPs showed selective sorption of only cationic dyes. The experimental data in this case are approximated by the Langmuir model of adsorption processes, which indicates the predominance of homogeneous and monolayer adsorption in the cases under consideration. Electrostatic interactions play the main role in the dye adsorption by $\text{Fe}_3\text{O}_4@\text{C}$ NPs.